

Structure and Function of the Photosynthetic Reaction Center from *Rhodobacter sphaeroides*¹

U. Ermler,² H. Michel,² and M. Schiffer³

Received September 29, 1993; accepted October 5, 1993

The three-dimensional structure of the photosynthetic reaction center from *Rhodobacter sphaeroides* is described. The reaction center is a transmembrane protein that converts light into chemical energy. The protein has three subunits: L, M, and H. The mostly helical L and M subunits provide the scaffolding and the finely tuned environment in which the chromophores carry out electron transfer. The details of the protein–chromophore interactions are from studies of a trigonal crystal form that diffracted to 2.65-Å resolution. Functional studies of the multi-subunit complex by site-specific replacement of key amino acid residues are summarized in the context of the molecular structure.

KEY WORDS: Photosynthetic reaction center; *Rhodobacter sphaeroides*; x-ray crystallography; protein structure; membrane protein electron transport; proton transport.

INTRODUCTION

The photosynthetic reaction center protein complex (RC) is the central component in the conversion of light energy to chemical energy in purple bacteria. It carries out a light-induced charge separation across the protein complex mediated by its chromophores. After absorption of a photon by a pair of bacteriochlorophyll (Bchl) molecules (the “special pair”) located close to the periplasm, an electron is transferred via the L-side bacteriopheophytin (Bphe) and a so-called primary quinone to a secondary quinone. After two such steps, the reduced secondary quinone takes up two protons from the cytoplasm and diffuses out of the RC. Another multiple subunit complex, the cytochrome *bcl* complex, transfers the electrons and protons of the reduced quinone to the periplasm

where the electrons are shuttled back by a soluble cytochrome *c*₂ to the reaction center. The stored energy of the generated proton gradient can be transformed by the protein complex ATP synthase to ATP.

The structure and function of the photosynthetic reaction centers from different organisms have been the focus of intensive investigation. Most advanced is our knowledge of the reaction centers from the purple bacteria and the green aerobic bacteria. The amino acid sequence of reaction centers from five of these bacteria are known: these are the RCs from the purple bacteria *Rhodobacter (Rb.) capsulatus* (Youvan *et al.*, 1984), *Rb. sphaeroides* (Williams *et al.*, 1983, 1984, 1986), *Rhodopseudomonas (Rps.) viridis* (Michel *et al.*, 1985, 1986a; Weyer *et al.*, 1987), *Rhodospirillum (Rs.) rubrum* (Belanger *et al.*, 1988), and the green aerobic bacteria *Chloroflexus aurantiacus* (Ovchinnikov *et al.*, 1988a,b; Shiozawa *et al.*, 1989). The comparison of these homologous sequences allows the identification of residues that are important for the structural integrity and function of the complex. Further, molecular biology techniques were developed for site-specific replacement of residues in three of the organisms: *Rb. capsulatus* (Youvan *et al.*, 1985), *Rb. sphaeroides* (Farchaus and Oesterhelt, 1989; Nagarajan *et al.*, 1990; Paddock *et*

¹This work was supported in part by the U.S. Department of Energy, Office of Health and Environmental Research, under Contract No. W-31-109-ENG-38 and by Public Health Service Grant GM36598.

²Max-Planck-Institut für Biophysik, Abt. Molekulare Membranbiologie, Heinrich-Hoffmann-Str. 7, D-6000 Frankfurt/M 71, Germany

³Center for Mechanistic Biology and Biotechnology, Argonne National Laboratory, Argonne, Illinois 60439.

al., 1989; Takahashi *et al.*, 1990), and *Rps. viridis* (Laussermair and Oesterhelt, 1992). This technique proved to be very effective for probing the function of specific residues. The three-dimensional structure has been determined by x-ray crystallography for the RCs from *Rps. viridis* (Deisenhofer and Michel, 1989) and *Rb. sphaeroides* (Feher *et al.*, 1989; Chang *et al.*, 1991; Ermler *et al.*, 1992).

The *Rps. viridis* RC has four protein subunits: the L, M, and H chains and a four-heme cytochrome. It contains four bacteriochlorophyll *b* molecules, two bacteriopheophytin *b* molecules, a menaquinone, an ubiquinone, a nonheme iron atom, and a carotenoid molecule (1,2-dihydroneurosporene). The *Rb. sphaeroides* RC has only three protein subunits, the L, M, and H chains. It contains four bacteriochlorophyll *a* molecules, two bacteriopheophytin *a* molecules, two ubiquinones, a nonheme iron atom, and a carotenoid (spheroidene) molecule. (The R26 mutant is missing the carotenoid.) The L chain has 273 amino acids in *Rps. viridis* and 281 amino acids in *Rb. sphaeroides*. The eight additional residues in the *Rb. sphaeroides* L chain are located at its C-terminal end; 59% of the amino acids of the L chains are identical in the two structures (Williams *et al.*, 1984; Michel *et al.*, 1986a). The M-chain in *Rps. viridis* RC has 323 amino acids; it has 18 extra residues at its C-terminal end compared with *Rb. sphaeroides*. The extra chain segment in *Rps. viridis* is used to anchor the cytochrome subunit. The M chain in *Rb. sphaeroides* has 307 residues, with two single amino acid insertions compared with the *Rps. viridis* M chain; one insertion is before the A helix and the other before the B helix. However, throughout this work the numbering from *Rps. viridis* M chain is used. Fifty percent of the amino acids of the M chains of the two species are identical (Williams *et al.*, 1983; Michel *et al.*, 1986a). Although the lengths of the H chains are similar (260 residues in *Rb. sphaeroides* and 258 residues in *Rps. viridis*), the overall sequence identity is only 39%; several insertions and deletions of chain segments are required for optimal alignment of the two sequences (Michel *et al.*, 1985; Williams *et al.*, 1986).

The structure of the *Rb. sphaeroides* RC from the orthorhombic crystal form has been determined by two independent groups using 3-Å data (Feher *et al.*, 1989 and Chang *et al.*, 1991), and more recently, a structure from a trigonal crystal form that diffracts to 2.65 Å resolution has been determined and is being refined (Ermler *et al.*, 1992). In this paper, the details of the structure discussed are from the trigonal

crystal form, which is expected to be more accurate because of the higher resolution of the diffraction data.

SUMMARY OF CRYSTALLIZATION CONDITIONS, STRUCTURE DETERMINATION, AND REFINEMENT OF THE RC STRUCTURES

***Rps. viridis* RC** (Deisenhofer and Michel, 1989). Crystals were grown from 2.2–2.4 M ammonium sulfate, in the presence of *N,N*-dimethyldodecyl amine-*N*-oxide (LDAO) and 3% heptane-1,2,3-triol. The unit cell is tetragonal $P4_32_12$ with dimensions $a = b = 223.5 \text{ \AA}$, $c = 113.6 \text{ \AA}$. Data were collected at the synchrotron source in Hamburg (DESY) at 0°C. Five different heavy atom derivatives were used to calculate the protein phases to 3 Å. After solvent flattening, the model of the complex was built and was refined using 2.3-Å data with the programs PROTEIN, EREF, and TNT (Deisenhofer *et al.*, 1985; Tronrud *et al.*, 1987; Deisenhofer and Michel, 1989). The *R* factor is 19.3% for 95,762 reflections to 2.3-Å resolution. The mean coordinate error for 10,288 nonhydrogen atoms was estimated to be 0.26 Å from a Luzzati plot (Luzzati, 1952).

***Rb. sphaeroides* R26 RC** (Allen *et al.*, 1986, 1987; Yeates *et al.*, 1988). The protein was isolated with LDAO and crystallized with PEG 4000 in the presence of LDAO, approximately 0.5 M NaCl, 15 mM Tris (pH 8), and 3.9% heptanetriol. After the crystals were grown, the LDAO was exchanged for octyl β ,*D*-glucoside. The unit cell is orthorhombic $P2_12_12_1$ with dimensions $a = 138.0 \text{ \AA}$, $b = 77.5 \text{ \AA}$, and $c = 141.8 \text{ \AA}$. Data were collected at the synchrotron source at Brookhaven. The structure was determined by molecular replacement using the partially refined coordinates of the *Rps. viridis* RC from 1985 (Deisenhofer *et al.*, 1985). Refinement was carried out using PROLSQ (Hendrickson, 1985). The *R* factor was 24% for 23,349 reflections to 2.8-Å resolution. The mean coordinate error was estimated to be 0.5 Å from Read's Q_A plot (Read, 1986). For the comparisons, published information about the structure was used.

***Rb. sphaeroides* R26 RC** (Chang *et al.*, 1985). The protein was isolated with octyl β ,*D*-glucoside and crystallized with PEG 4000 in the presence of octyl β ,*D*-glucoside, 0.3 M NaCl, and 10 mM Tris (pH 8). The unit cell is orthorhombic $P2_12_12_1$ with dimen-

sions $a = 142.2 \text{ \AA}$, $b = 139.6 \text{ \AA}$, and $c = 78.7 \text{ \AA}$. Data were collected at the synchrotron source at Stanford (SSRL). The structure was determined by molecular replacement (Chang *et al.*, 1986) using the partially refined coordinates of the *Rps. viridis* RC (Deisenhofer *et al.*, 1985). The refinement was carried out with the programs PROLSQ (Hendrickson, 1985) and TNT (Tronrud *et al.*, 1987). The R factor was 22% for 13,493 reflections to 3.1- \AA resolution (Chang *et al.*, 1991). The mean coordinate error was estimated to be 0.5 \AA from a Luzzati plot.

Rb. sphaeroides wild-type RC (Buchanan *et al.*, 1993). The protein was isolated with LDAO and crystallized by vapor diffusion against 1.3–1.5 M potassium phosphate, in the presence of 0.09% LDAO, 1.0% 1,4-dioxane, 3.4% 1,2,3-heptanetriol, and 1.0 M potassium phosphate, pH 7.8. The unit cell is trigonal $P3_121$ with dimensions $a = b = 141.4 \text{ \AA}$, $c = 187.2 \text{ \AA}$. Data were collected at the synchrotron source in Hamburg (DESY). The structure was determined by molecular replacement using the previously determined *Rb. sphaeroides* structure (Yeates *et al.*, 1988). The refinement was carried out by X-PLOR (Brünger *et al.*, 1987). The R factor was 18.6% for 56,141 reflections to 2.65- \AA resolution. The mean coordinate error was estimated to be 0.28 \AA from a Luzzati plot.

DESCRIPTION OF THE COMPLEX

The RC from *Rb. sphaeroides* is a complex formed from three protein subunits (the L, M, and H chains) and eight chromophores (Fig. 1). Embedded in the L and M chains are the nonprotein cofactors. There are two bacteriochlorophyll molecules (BC_{LP} and BC_{MP}) that form the “special” pair, two monomeric bacteriochlorophylls (BC_{LA} and BC_{MA}), two bacteriopheophytins (BP_L and BP_M), and two ubiquinones (Q_A and Q_B). The complex also contains a nonheme Fe^{2+} atom.

Two principal evolutionary “forces” combined are responsible for the RC architecture. First, the energy-transducing role of this protein complex defined the composition, location, and microenvironmental chemistries of the chromophores, as well as other constituents of the electron transport system. Second, the fact that the electron must be transported across a barrier requires the RC to span the barrier and to possess surface properties compatible with multiple environments.

The RC is a transmembrane protein that is designed to pass through and function in three different environments. There are two distinct environments within the membrane bilayer itself. The center portion of the bilayer, about 30 \AA in width, is hydrophobic (lipophilic). The two surfaces of the bilayer are formed from polar lipid head groups approximately 5 \AA in width. Outside the membrane in the cytoplasm or in the periplasm, the environment is polar. Based on alignment with a model membrane, the L and M subunits are flush with the membrane surface on the periplasmic side. The bulk of the H subunit is located in the cytoplasm. The quinone head groups are at the level of the membrane head groups, and the bacteriochlorophylls and bacteriopheophytins are at the level of the hydrophobic part of the bilayer. While the cytoplasmic portion of the H subunit has many polar and charged residues, the charged residues in the L and M chains are distributed near the lipid head groups of the membrane surfaces.

The L and M chains are transmembrane proteins with homologous structures and sequences. Each chain contains five transmembrane helices (A, B, C, D, E) and other short helical segments (Deisenhofer *et al.*, 1985). The transmembrane helices are the most striking feature of the structure (Fig. 2). A local, non-crystallographic, two-fold axis relates the M and L subunits. The H chain has only one transmembrane helical segment at its N-terminal end; most of the H subunit is located on the cytoplasmic side of the membrane. The cytoplasmic part of the H chain is like a globular, soluble protein with a polar exterior and hydrophobic interior. It has several antiparallel β -sheets and one α -helical segment. The local two-fold axis of the complex does not apply to the H chain. The complex can function *in vitro* without the H chain, though with diminished efficiency (Debus *et al.*, 1985). The H chain does not participate directly in the accommodation of the chromophores, but it increases the barrier between Fe^{2+} and quinones with respect to the cytoplasm. The H chain is considered to be important in the proper assembly of the complex in the membrane (Chory *et al.*, 1984).

The tertiary structure of the RC complex is stabilized by hydrophobic interactions between the L and M chains, by interactions of the pigments with each other and with the L and M chains, by residues from the L and M chains that coordinate to the Fe^{2+} , by hydrogen bonds and salt bridges that are formed between the L and M chains and the H chain, and

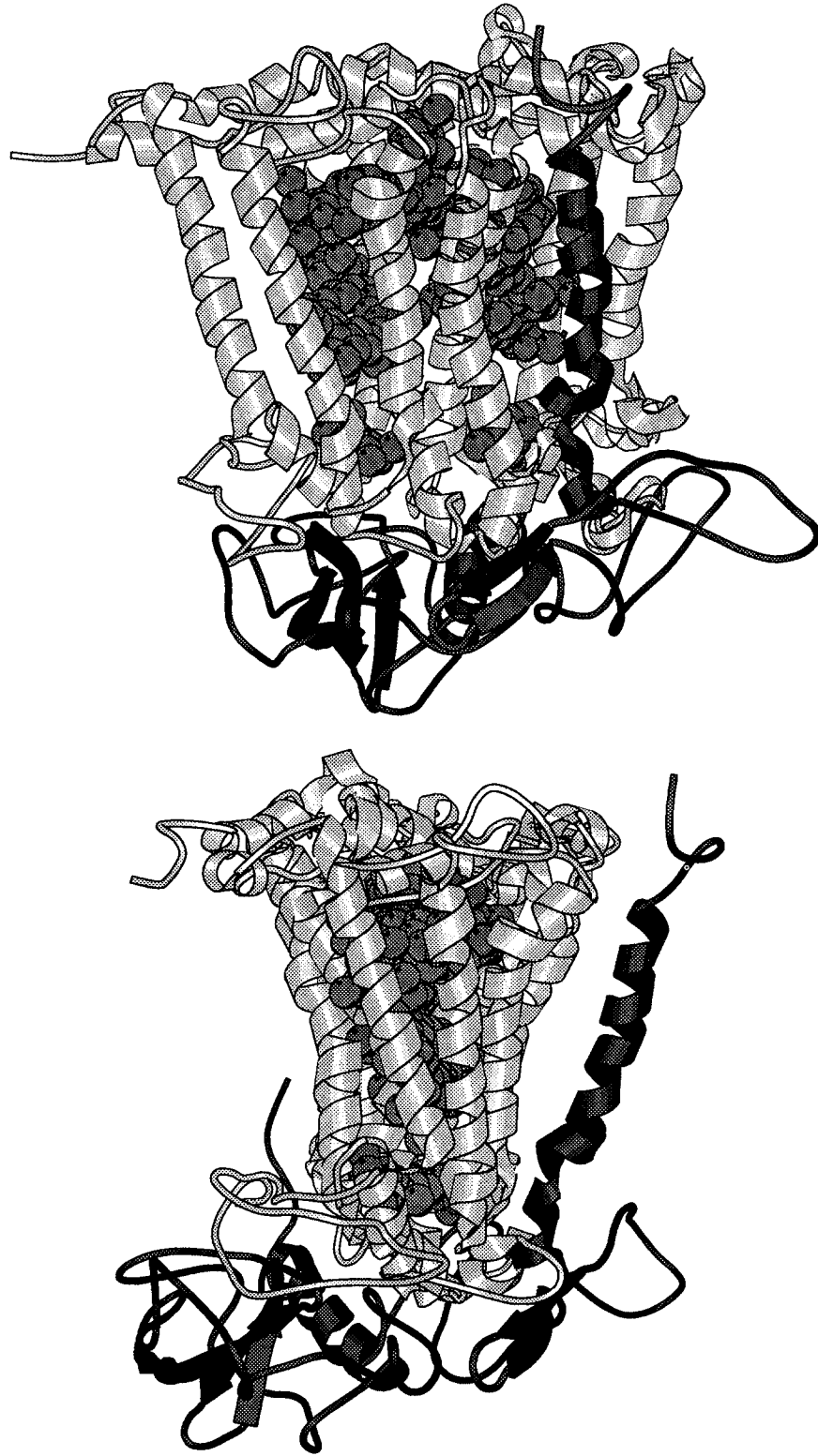


Fig. 1. Two views of the *Rb. sphaeroides* complex using Molscript (Kraulis, 1991). The H chain is shown in a darker shade; the chromophores are shown in space-filling representation.

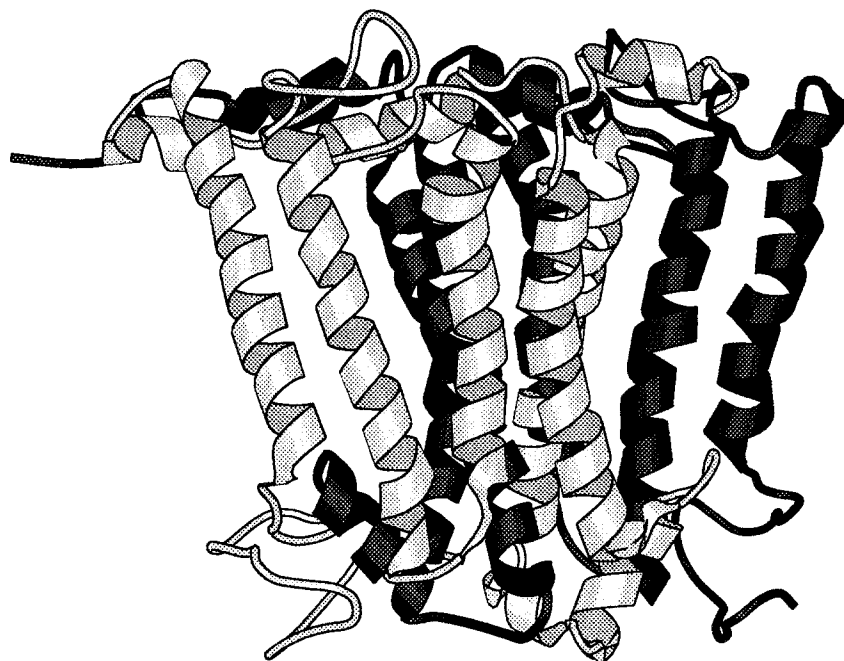


Fig. 2. The symmetrical arrangement of the L and M transmembrane chains is illustrated. The L-chain is in a darker shade.

possibly by electrostatic forces between the ends of helices. The hydrogen bonds between the L and M chains are near the periplasmic surface and also in the transmembrane region. Approximately one-third of the salt bridges are interchain bridges between the H subunit and the M and L subunits. The topology of the complex is such that the L and M chains, the four bacteriochlorophylls, and the two bacteriopheophytins are required together for its assembly. The bacteriochlorophylls of the special pair are completely buried with the exception of the last few atoms of the phytol tails. The phytol tails of the monomeric bacteriochlorophylls and the bacteriopheophytins are in contact with the membrane. The macrocycle of the M-side bacteriopheophytin is completely buried, while 3% of the L-side one is in contact with the membrane. The most exposed chromophores, in which about 10% of the macrocycles are in contact with the membrane or with the detergent in the crystal, are the monomeric bacteriochlorophylls.

HELICAL SEGMENTS OF THE L AND M CHAINS

The transmembrane helices of the RC are characterized by the absence of charged residues in the middle of the helical regions. In each helix, there

exists a segment of at least 16 residues uninterrupted by Glu, Asp, Lys, Arg, or His residues. No other segment of the RC molecule has this characteristic.

There are helical regions on the periplasmic surface of both the L and M subunits. Because of their location, these are amphipathic helices that have a well-defined hydrophobic side and a well-defined polar side. The polar side points toward the periplasm and can form the surface of contact with the soluble cytochrome c_2 molecule. On the cytoplasmic side of the complex, helical segments in both subunits form parts of the quinone binding sites. The M subunit has an additional, short helical segment located on the cytoplasmic side of the Fe^{2+} atom.

There are kinks in helices C and E of both the L and M chains. The presence of a proline near the C-terminal end of the C helices causes a wider turn and a change in direction of the helix in the last few turns. In the E helix, it is not a proline but the special pair bacteriochlorophylls near the middle of the helix that appear to cause the helices to kink away from the special pair.

DESCRIPTION OF PIGMENT LOCATIONS

The RC complex appears to be a very simple

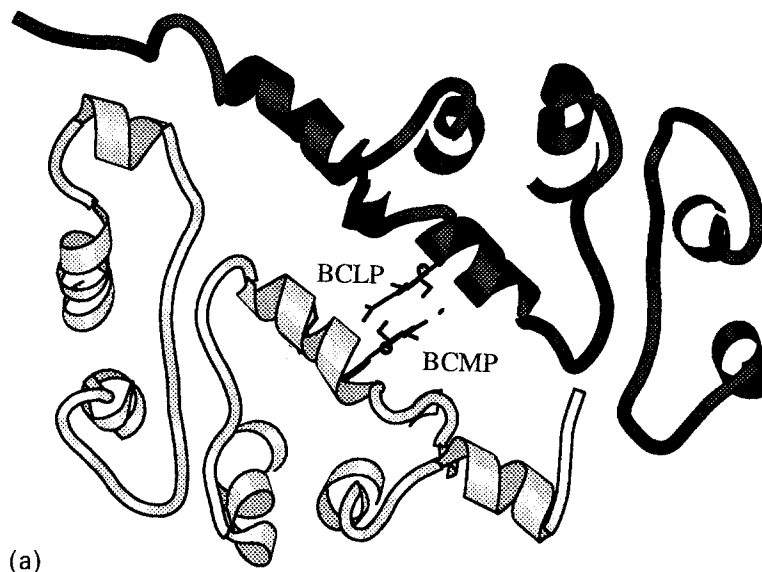


Fig. 3. Sections through the reaction center perpendicular to the local twofold axis, viewed from the periplasmic side of the complex. Protein backbone and the cofactors are shown using Molscript (Kraulis, 1991); the L chain is in a darker shade. (a) Section close to the periplasmic side of the complex; it includes the top of the special pair. (b) Section includes the monomeric and the special pair Bchl's. The special pair is close to parallel to the twofold axis of the complex (z axis) and makes an angle of 37° with the x axis. It can be seen in this section that monomeric Bchl's are equally distant from both members of the special pair, and together they form a tetramer of Bchl's. (c) The Bphe's are shown in this section. The line connecting their centers makes an angle of 18° with the x -axis. They are separated from each other by the D and E helices from each subunit. (d) This section illustrates the positions of the quinones and iron atom. The line that connects the centers of the quinones makes an angle of -10° with the x axis. In comparing the different sections, it can be seen that the bacteriopheophytins and quinones do not superimpose when viewed along the z axis. The orientations and curvatures of the transmembrane helices are such that the space between them is expanded to accommodate the Bchl's.

structure because of the local twofold axis and the five helical segments of the L and M subunits that are nearly parallel to the two-fold axis. But the description of the molecule is made difficult by the twist of the transmembrane helical segments. To describe the relative positions of the pigments, we defined a coordinate system where the x axis connects the A_L and A_M helices at the level of the monomeric BChl's. The positive direction is toward the A_L helix. The two-fold axis direction is defined as the z axis. Four sections through the RC, perpendicular to the two-fold axis, are shown in Fig. 3. The "top" of the complex, facing the periplasm, is perpendicular to the two-fold axis and is parallel to the membrane.

The special pair and the two monomeric bac-

teriochlorophylls form a tetramer. The centers of BC_{LA} and BC_{MA} by definition lie on the x axis. The planes of the special pair bacteriochlorophylls are approximately parallel with the line connecting the C helices and make an angle of 37° with the x axis. BC_{LP} is closer to the protein on the L side, and BC_{MP} is closer to the protein on the M side. The monomeric Bchl's are about equidistant from both Bchl's of the special pair and in van der Waals contact with both. The monomeric Bchl's are separated from each other by the special pair.

While the macrocycles of the special pair are nearly parallel to the two-fold axis of the complex, the macrocycles of the monomeric Bchl are more closely parallel with the membrane plane. BC_{LA} is

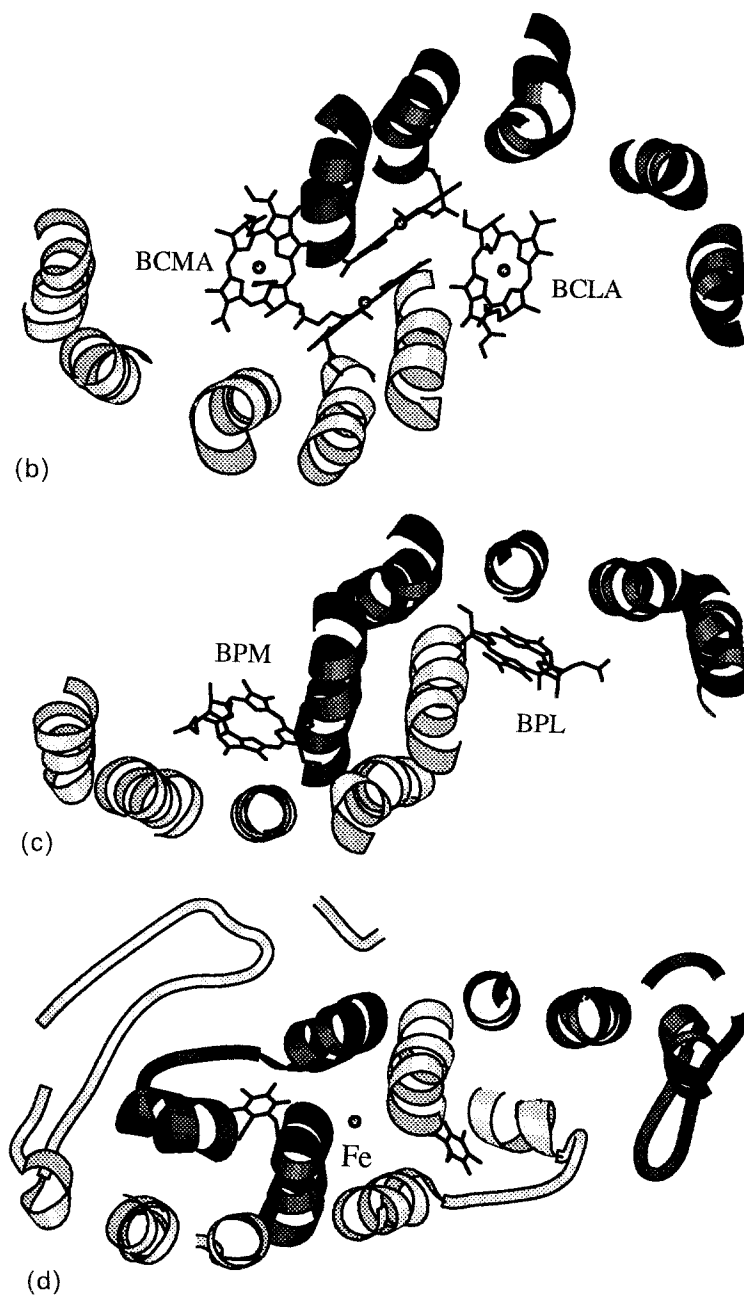


Fig. 3. Continued.

“under” and approximately parallel to the CD helix on the L side, while BC_{MA} is “under” and approximately parallel to the CD helix on the M side. Though the center of mass of the special pair and the monomeric Bchl’s are not at the same level in the membrane, their phytyl tails begin at approximately the same level. This is the result of the different tilts of the macrocycles relative to the plane of the membrane.

The macrocycles of the two chlorophylls forming

the special pair are closely parallel, and the atoms of ring I of each overlap with each other. The carbon atom (C3B) of each Bchl overlaps the nitrogen atom (NB) of the other Bchl of the special pair. This arrangement places the acetyl carbonyl, an extension of the π system of one macrocycle, under the π system of the other macrocycle. The resulting angle between the Qy direction of BC_{LP} and BC_{MP} is 141° . The Qy directions of the monomeric Bchl’s are almost parallel

to that of the special pair; BC_{LA} is parallel to BC_{MP} , and BC_{MA} is parallel to BC_{LP} . The angle made by the Qy directions of BC_{LA} and BC_{MA} is 144° . Ring III of BC_{LA} is close to ring I of BC_{MP} , and ring III of BC_{MA} is close to ring I of BC_{LP} .

The pheophytins are "under" the monomeric Bchl's on the L and M side and are separated from each other by the D and E helices of the protein. The interactions of the Bphe with the monomeric Bchl resembles that of the special pair. They form a distorted dimer, and their closest approach is at ring I of both macrocycles. The Qy directions of the Bphe's are close to parallel to the two-fold axis. A line drawn through the centers of the Bphe's makes an angle of 18° with the projection of the x axis. This line passes between the A and B helices at the level of the Bphe's.

The line connecting the centers of the quinones makes an angle of -10° with the projection of the x axis. While both the quinones and the BPhe's are under the monomeric Bchl's, they are not directly under each other. The quinones are under ring III and the BPhe's are under rings I and II of the monomeric Bchl's.

DETAILS OF CHROMOPHORE-PROTEIN INTERACTIONS

A remarkable property of the RC complex is that in spite of its symmetry, the electron transfer occurs through only one side of the complex (e.g., see Michel-Beyerle *et al.*, 1988), through the L-side bacteriopheophytin (BP_L) to Q_A . The electron does not seem to pass through the M-side bacteriopheophytin (BP_M). The unidirectionality of electron transport must be caused by the different protein environments of the chromophores, but how this is achieved is not known at present. The most obvious are the differences in charged and/or polar residues on the two sides that are capable of forming hydrogen bonds with the chromophores, thereby altering their environments. The protein matrix affects the relative geometry, angles, and distances of the chromophores relative to each other in the two branches. It is much more difficult to identify the individual amino acids responsible for the detailed geometry of the molecule. Spectroscopic techniques that elucidate the electron transfer pathway rely on the different spectral properties of the bacteriopheophytins; these properties in turn are modulated by the nature of the protein that

surrounds the pigments (e.g., hydrogen bonds, nearby charged groups, etc.).

Residues M208 and L181 are located near the center of the complex; each residue is in van der Waals contact with four chromophores (Tiede *et al.*, 1988). In *Rps. viridis*, *Rb. sphaeroides*, *Rb. capsulatus*, and *Rs. rubrum* M208, the residue that is close to the L-side of the complex is a Tyr residue, while the symmetry-related residue is a Phe. Several groups replaced these residues in *Rb. sphaeroides* (Nagaranjan *et al.*, 1990; Gray *et al.*, 1990) and *Rb. capsulatus* (Chan *et al.*, 1991; DiMugno *et al.*, 1992). While there is no change in the direction of the electron flow, differences were found in the rate of the electron transfer from the special pair to the bacteriopheophytin and the redox potential of the special pair. Polar and aromatic residues at position M208 increase the rate of electron transfer. On the other hand, Phe L181 can be replaced by the polar residues Tyr, His, Thr, Glu, or Lys. Interestingly, when a Tyr residue is present at both the L181 and M208 positions, the first electron transfer step is faster than in the wild type (Chan *et al.*, 1991). Substitution of His at M208 significantly changes the absorption spectrum of BP_L , while Lys at position L181 changes the absorption spectrum of BC_{MA} (Schiffer *et al.*, 1992b).

The special pair is located close to the periplasmic side of the complex in a hydrophobic environment formed by residues of the L and M subunits. The planes of their macrocycles are nearly parallel to each other and to the local two-fold axis. The special pair is in contact with residues from the C, D, E, and CD helices of the L and M subunits, respectively.

The central Mg atoms of BC_{LP} and BC_{MP} in both RCs are liganded to the NE2 atoms of histidines L173 and M200 of the D helices. These His residues, which coordinate to the Mg^{2+} , have been replaced by Gln, Phe, and Leu residues (Bylina and Youvan, 1988; McDowell *et al.*, 1991). Although Gln does not seem to have an effect, the hydrophobic residues Leu and Phe cause the incorporation of bacteriopheophytin instead of bacteriochlorophyll into the sites.

In *Rps. viridis*, the ring I acetyl carbonyl oxygens of BC_{LP} and BC_{MP} are hydrogen-bonded to His L168 and Tyr M195, respectively. The *Rb. sphaeroides* structure shows that a similar hydrogen bond is formed between the conserved His L168 (NE2) and the ring I acetyl of BC_{LP} . In contrast, the residue at the symmetry-related position on the M-side, Phe M195, cannot form a hydrogen bond to BC_{MP} . Thus, the symmetry in hydrogen-bonding to the ring

I acetyl groups in the bacteriochlorophyll dimer of *Rps. viridis* is not preserved in *Rb. sphaeroides*. No other hydrogen bond to the special pair is found in *Rb. sphaeroides*. In *Rps. viridis*, Thr L248 forms a hydrogen bond with the keto carbonyl of ring V of BC_{LP}, while in *Rb. sphaeroides*, L248 is a Met residue that cannot form a hydrogen bond. However, a weak polar contact is observed between the ester carbonyl and the side chain of Cys L247 in *Rb. sphaeroides*; in *Rps. viridis*, this is a Gly residue. The breaking of the hydrogen bond in *Rb. sphaeroides* by replacing His L168 with Phe increases the midpoint potential of the special pair (Murchison *et al.*, 1993).

The bacteriochlorophyll monomers BC_{LA} and BC_{MA} interact with the special pair and neighboring bacteriopheophytins. Amino acid residues from the B, C, D, and CD helices of the L and M subunits surround the monomers. Two histidines, L153 and M180 of the CD periplasmic helix of both *Rps. viridis* and *Rb. sphaeroides* RCs, are liganded to the central Mg²⁺ atoms of BC_{LA} and BC_{MA}, respectively. His L153 was replaced by Ser, Thr, Arg, or Leu, and His M180 was replaced by Ser, Leu, or Arg (Bylina *et al.*, 1990). The Ser and Thr mutants retain the bacteriochlorophyll, while the effect of the Leu mutation is not clear because it was not possible to isolate the RCs. Only the Arg mutation made the complex photosynthetically incompetent. No hydrogen bond between the protein matrix and the bacteriochlorophyll monomers was observed in either RC.

Each macrocycle of the bacteriopheophytins (BP_L and BP_M) is located approximately at the center of the C and E helices. BP_L is oriented parallel to the D helix of the M chain and BP_M is oriented parallel to the D helix of the L chain. BP_L and BP_M are in contact with residues from the D, E, B, and C membrane-spanning helices of the L and M subunits. The only ionizable residue near the macrocycles of the chromophores is the conserved residue Glu L104. The side chain of Glu L104 is assumed to be protonated (Michel *et al.*, 1986b) and forms a hydrogen bond with the keto carbonyl of ring V of BP_L. Glu L104 in *Rb. capsulatus* RCs has been replaced by Gln, Lys, or Leu residues (Bylina *et al.*, 1988). In these mutants, the rates of electron transfer along the L-pathway were only slightly modified (less than a factor of 2), and the yield of light-induced electron transfer along the L-pathway was unaltered. Leu at position L104 causes a blue shift in the absorption spectrum of BP_L, identifying this bacteriopheophytin as the photoactive

one. In *C. aurantiacus*, Glu L104 is replaced by a noncharged Gln residue (Ovchinnikov *et al.*, 1988a; Shiozawa *et al.*, 1989).

Trp M250 is a conserved residue that is located between BP_L and Q_A. Its position and orientation are similar in both *Rps. viridis* and *Rb. sphaeroides* RCs; it forms a hydrogen bond with Thr M220. Trp M250 has been replaced by Phe, Leu, Met, Val, Glu, and Arg in *Rb. capsulatus* RC (Coleman and Youvan, 1990) and by Tyr and Phe in *Rb. sphaeroides* RC (Stilz *et al.*, 1993). Only the organisms that have Phe or Tyr substitution can grow photosynthetically. The other substitutions lower the affinity of the quinone for the Q_A site, but the isolated RCs can function with added quinone. The rate of electron transfer from the bacteriopheophytin to the quinone is slowed in these mutants.

The quinone Q_A is located near the BP_L and close to the cytoplasmic side of the RC. Q_A interacts with residues of the M subunit from the D and E membrane-spanning helices as well as with the DE helix. In *Rps. viridis*, the two oxygens of the Q_A ring (menaquinone) are hydrogen-bonded to the peptide nitrogen of Ala M258 and the side chain of His M217, respectively. Though in *Rb. sphaeroides*, the Q_A site is occupied by a ubiquinone, its position is like that found in the *Rps. viridis* RC.

Near the Q_B site, residues from the M and H chains are present in addition to residues from the D, DE, and E helices of the L subunit. In the structures of *Rb. sphaeroides* RC based on an orthorhombic crystal form and in *Rps. viridis*, there are hydrogen bonds between the two carbonyl oxygens of the Q_B ring and the side chain of His L190 and Ser L223. In the *Rb. sphaeroides* RC structure derived from the trigonal crystal form, the quinone position is displaced approximately 5 Å. Although the profile of the Q_B binding site is conserved, the quinone is located closer to the entrance of the pocket, and it only forms a hydrogen bond with the protein backbone. This quinone site does not appear to be highly occupied. The role of the second Q_B binding site for the electron and proton transfer process is not understood at the present time.

The residues that constitute the Q_B site make it far more polar than the Q_A site. The lower polarity of the Q_A pocket may contribute to the stronger binding of Q_A and the modification of its redox properties compared to Q_B. The Q_A site has no charged residues, but it tolerates replacement of Ala 247 by an Asp residue (Schiffer *et al.*, 1992b). The Q_B site con-

tains charged residues at positions L212 and L213, which are shown to be involved in proton transfer in wild-type *Rb. sphaeroides* (Paddock *et al.*, 1989; Takahashi and Wraight, 1992; Okamura and Feher, 1992). However, studies of *Rb. capsulatus* mutants have shown that one charged residue, Asp L213, or an Asp residue at alternate positions (L225, M43), or the replacement of Arg M231 with a Leu residue is sufficient for photosynthetic growth (Hanson *et al.*, 1993). In the *Rps. viridis* and *Rs. rubrum* RCs, L213 is an Asn, but M43 is Asp. Ser L223 is part of the proton transfer pathway in both *Rb. capsulatus* and *Rb. sphaeroides* (Coleman and Youvan, 1990; Paddock *et al.*, 1990) and in *Rps. viridis* (Leibl *et al.*, 1993). Mutation of Ser L223 to Ala seems to prevent the second electron transfer by preventing proton uptake.

The side chain of Tyr L222 is too far away to form a hydrogen bond with Q_B; it forms a hydrogen bond with the peptide carbonyl oxygen of M43. When Tyr L222 was replaced by Phe in the *Rps. viridis* RC (Michel *et al.*, 1990), a major rearrangement of part of the M-chain (M25–M55) occurs. The indole ring of Trp M266 is near the tail of Q_A, while the equivalent smaller aliphatic residue on the L chain, Leu L232, is close to the tail of Q_B. The smaller residues in the Q_B site might allow for the diffusion of the protonated quinone from the complex.

The nonheme iron (Fe²⁺) lies approximately on the two-fold symmetry axis relating the cofactors of the L and M side between the Q_A and Q_B rings. Fe²⁺ is liganded to the NE2 atoms of the side chains of four histidine residues from the D and E helices (L190, L230, M217, and M264), and one glutamic acid from the DE helix (M232) acts as a bidentate ligand. The two imidazole rings of histidines L190 and M217 are located between the Fe and the Q_A and Q_B rings, respectively. These polar interactions between the Fe and the ligands of the L and M subunits may play an important role in stabilizing the tertiary structure of the RC complex.

FUTURE DIRECTIONS

The main interest in the RC complex up to now has been in the field of photosynthesis because of its electron and proton transfer capabilities. The RC is also the first transmembrane protein for which a high-resolution atomic structure is known; therefore, it

serves as a model for other transmembrane proteins such as receptors. Certain amino acid residues such as Trp appear to have a specialized function in these proteins (Deisenhofer and Michel, 1989; Schiffer *et al.*, 1992a). The effect on the stability and/or assembly of this multi-subunit complex can be probed by site-specific mutagenesis, and the chromophores can be used as reporter groups through analysis of their spectroscopic properties.

ACKNOWLEDGMENTS

M.S. would like to thank colleagues C.-H. Chang, D. K. Hanson, O. El-Kabbani, J. R. Norris, D. Tiede, J. Tang, and U. Smith, on whose work part of this summary is based, and L. L. Ho for making the figures. U. E. and H. M. thank S. Buchanan and G. Fritzsche for their contributions to the structure of the trigonal form of the *Rb. sphaeroides* RC and I. Sinning for her contribution to the mutant structures of the *Rps. viridis* RC.

REFERENCES

- Allen, J. P., Feher, G., Yeates, T. O., Rees, D. C., Deisenhofer, J., Michel, H., and Huber, R. (1986). *Proc. Natl. Acad. Sci. USA* **83**, 8589–8593.
- Allen, J. P., Feher, G., Yeates, T. O., Komiya, H., and Rees, D. C. (1987). *Proc. Natl. Acad. Sci. USA* **84**, 6162–6166.
- Belanger, G., Berard, J., Corriveau, P., and Gingras, G. (1988). *J. Biol. Chem.* **263**, 7632–7638.
- Brünger, A. T., Kuriyan, J., and Karplus, M. (1987). *Science* **235**, 458–460.
- Buchanan, S. K., Fritzsche, G., Ermler, U., and Michel, H. (1993). *J. Mol. Biol.* **230**, 1311–1314.
- Bylina, E. J., Kirmaier, C., McDowell, L., Holten, D., and Youvan, D. C. (1988). *Nature (London)* **336**, 182–184.
- Bylina, E. J., and Youvan, D. C. (1988). *Proc. Natl. Acad. Sci. USA* **85**, 7226–7230.
- Bylina, E. J., Kolaczowski, S. V., Norris, J. R., and Youvan, D. C. (1990). *Biochemistry* **29**, 6203–6210.
- Chan, C.-K., Chen, L. X.-Q., DiMagno, T. J., Hanson, D. K., Nance, S. L., Schiffer, M., Norris, J. R., and Fleming, G. R. (1991). *Chem. Phys. Lett.* **176**, 366–372.
- Chang, C.-H., Schiffer, M., Tiede, D., Smith, U., and Norris, J. (1985). *J. Mol. Biol.* **186**, 201–203.
- Chang, C.-H., Tiede, D., Tang, J., Smith, U., Norris, J., and Schiffer, M. (1986). *FEBS Lett.* **205**, 82–86.
- Chang, C.-H., El-Kabbani, O., Tiede, D., Norris, J., and Schiffer, M. (1991). *Biochemistry* **30**, 5352–5360.
- Chory, J. T., Donohue, J., Varga, A. R., Staehelin, L. A., and Kaplan, S. (1984). *J. Bacteriol.* **159**, 540–554.
- Coleman, W. J., and Youvan, D. C. (1990). *Annu. Rev. Biophys. Biophys. Chem.* **19**, 333–367.

- Debus, R. J., Feher, G., and Okamura, M. Y. (1985). *Biochemistry* **24**, 2488–2500.
- Deisenhofer, J., Epp, O., Miki, R., Huber, R., and Michel, H. (1985). *Nature (London)* **318**, 618–624.
- Deisenhofer, J., and Michel, H. (1989). *EMBO J.* **8**, 2149–2169.
- DiMugno, T. J., Rosenthal, S. J., Xie, X., Du, M., Chan, C.-K., Hanson, D. K., Schiffer, M., Norris, J. R., and Fleming, G. R. (1992). In *The Photosynthetic Bacterial Reaction Center II* (Breton, J., and Vermeglio, A., eds.), Plenum Press, New York, pp. 209–217.
- Ermiler, U., Fritzsche, G., Buchanan, S., and Michel, H. (1992). In *Research in Photosynthesis* (Murata, N., ed.), Kluwer, The Netherlands, pp. 341–347.
- Farchaus, J. W., and Oesterhelt, D. (1989). *EMBO J.* **8**, 47–54.
- Feher, G., Allen, J. P., Okamura, M. Y., and Rees, D. C. (1989). *Nature (London)* **339**, 111–116.
- Gray, K. A., Farchaus, J. W., Wachtveitl, J., Breton, J., and Oesterhelt, D. (1990). *EMBO J.* **9**, 2061–2070.
- Hanson, D. K., Tiede, D. M., Nance, S. L., Chang, C.-H., and Schiffer, M. (1993). *Proc. Natl. Acad. Sci. USA.*, **90**, 8929–8933.
- Hendrickson, W. (1985). *Methods Enzymol.* **115**, 252–270.
- Kraulis, P. J. (1991). *J. Appl. Crystallogr.* **24**, 946–950.
- Laussermair, E., and Oesterhelt, D. (1992). *EMBO J.* **11**, 777–783.
- Leibl, W., Sinning, I., Ewald, G., Michel, H., and Breton, J. (1993). *Biochemistry* **32**, 1958–1964.
- Luzzati, P.V. (1952). *Acta Crystallogr.* **5**, 802–810.
- McDowell, L. M., Gaul, D., Kirmaier, C., Holten, D., and Schenck, C. C. (1991). *Biochemistry* **30**, 8315–8322.
- Michel, H., Weyer, K. A., Gruenberg, H., and Lottspeich, F. (1985). *EMBO J.* **4**, 1667–1672.
- Michel, H., Weyer, K. A., Gruenberg, H., Dunger, I., Oesterhelt, D., and Lottspeich, F. (1986a). *EMBO J.* **5**, 1149–1158.
- Michel, H., Epp, O., and Deisenhofer, J. (1986b). *EMBO J.* **5**, 2445–2451.
- Michel, H., Sinning, I., Koepke, J., Ewald, G., and Fritzsche, G. (1990). *Biochim. Biophys. Acta* **1018**, 115–118.
- Michel-Beyerle, M. E., Plato, M., Deisenhofer, J., Michel, H., Bixon, M., and Jortner, J. (1988). *Biochim. Biophys. Acta* **932**, 52–70.
- Murchison, H. A., Alden, R. G., Allen, J. P., Peloquin, J. M., Taguchi, A. K. W., Woodbury, N. W., and Williams, J. C. (1993). *Biochemistry* **32**, 3498–3505.
- Nagarajan, V., Parson, W. W., Gaul, D., and Schenck, C. (1990). *Proc. Natl. Acad. Sci. USA* **87**, 7888–7892.
- Okamura, M. Y., and Feher, G. (1992). *Annu. Rev. Biochem.* **61**, 861–896.
- Ovchinnikov, Y. A., Abdulaev, N. G., Zolotarev, A. S., Schmuckler, B. E., Zargarov, A. A., Kutuzov, M. A., Telezhinskaya, I. N., and Levina, N. B. (1988a). *FEBS Lett.* **231**, 237–242.
- Ovchinnikov, Y. A., Abdulaev, N. G., Schmuckler, B. E., Zargarov, A. A., Kutuzov, M. A., Telezhinskaya, I. N., Levina, N. B., and Zolotarev, A. S. (1988b). *FEBS Lett.* **232**, 364–368.
- Paddock, M. L., Rongey, S. H., Feher, G., and Okamura, M. Y. (1989). *Proc. Natl. Acad. Sci. USA* **86**, 6602–6606.
- Paddock, M. L., McPherson, P. H., Feher, G., and Okamura, M. Y. (1990). *Proc. Natl. Acad. Sci. USA* **87**, 6803–6807.
- Read, R. J. (1986). *Acta Crystallogr. Sect. A* **42**, 140–149.
- Schiffer, M., Chang, C.-H., and Stevens, F. J. (1992a). *Protein Eng.* **5**, 213–214.
- Schiffer, M., Chan, C.-K., Chang, C.-H., DiMugno, T. J., Fleming, G. R., Nance, S., Norris, J., Snyder, S., Thurnauer, M., Tiede, D. M., and Hanson, D. K. (1992b). In *The Photosynthetic Bacterial Reaction Center II* (Breton, J., and Vermeglio, A., eds.), Plenum Press, New York, pp. 351–361.
- Shiozawa, J. A., Feick, R., Oesterhelt, D., and Lottspeich, F. (1989). *Eur. J. Biochem* **180**, 75–84.
- Stilz, H. U., Finkle, U., Holzappel, W., Lauterwasser, C., Zinth, W., and Oesterhelt, D. (1993). *Eur. J. Biochem.*, submitted.
- Takahashi, E., Maroti, P., and Wraight, C. A. (1990). In *Current Research in Photosynthesis* (Baltscheffsky, M., ed.), Kluwer, The Netherlands, pp. 169–172.
- Takahashi, E., and Wraight, C. A. (1992). *Biochemistry* **31**, 855–866.
- Tiede, D. M., Budil, D. E., Tang, J., El-Kabbani, O., Norris, J. R., Chang, C.-H., and Schiffer, M. (1988). In *The Photosynthetic Bacterial Reaction Center* (Breton, J., and Vermeglio, A., eds.), Plenum Press, New York, pp. 13–20.
- Tronrud, D. E., Ten Eyck, L. F., and Matthews, B. W. (1987). *Acta Crystallogr. Sect. A* **43**, 489–501.
- Weyer, K. A., Lottspeich, F., Gruenberg, H., Lang, F., Oesterhelt, D., and Michel, H. (1987). *EMBO J.* **6**, 2197–2202.
- Williams, J. C., Steiner, L. A., Ogden, R. C., Simon, M. I., and Feher, G. (1983). *Proc. Natl. Acad. Sci. USA* **80**, 6505–6509.
- Williams, J. C., Steiner, L. A., Feher, G., and Simon, M. I. (1984). *Proc. Natl. Acad. Sci. USA* **81**, 7303–7307.
- Williams, J. C., Steiner, L. A., and Feher, G. (1986). *Proteins* **1**, 312–325.
- Yeates, T. O., Komiya, H., Chirino, A., Rees, D. C., Allen, J. P., and Feher, G. (1988). *Proc. Natl. Acad. Sci. USA* **85**, 7993–7997.
- Youvan, D. C., Bylina, E. J., Alberti, M., Begusch, H., and Hearst, J. E. (1984). *Cell* **37**, 949–957.
- Youvan, D. C., Ismail, S., and Bylina, E. J. (1985). *Gene* **33**, 19–30.